Developmental Testbed Center (DTC) Project for the Air Force Weather Agency (AFWA)

Final Report of Annual Baseline GSI Experiments (Appendix Task)

February 2013

Index

1. Introduction

The Grid Point Statistical Interpolation (GSI) Data Assimilation System is a three dimensional variational (3D-Var) and hybrid data assimilation (DA) system currently used by various agencies as part of operational systems for both regional and global applications, including NCEP's Global Forecast System (GFS) System, North American Mesoscale Forecast System (NAM), and Hurricane WRF Forecast System (HWRF)), NASA's Global Forecast System as well as NOAA's Rapid Refresh System (RAP). The GSI is also a community research model with public access. The DTC provides code management and user support and facilitates code transitions from research to operations. The DTC releases an updated GSI code annually.

In the past, the baseline experiments were designed to test the new released code for AFWA applications with focus on testing the latest added capabilities. Since GSI is not yet implemented operationally at AFWA, following a discussion with AFWA, the DTC steered the baseline tests with the motivation to assist AFWA in determining an appropriate initial configuration of GSI for operational implementation. The baseline experiments were performed using a functionally-similar operational environment and complement the AFWA real-time pre-operation parallel GSI runs. The AFWA parallel runs bring in updates and changes periodically and focus on evaluating the overall performance of GSI. However, the DTC performs both real-

time and retrospective GSI runs and focuses on testing incremental changes. The real-time runs are used to sync the test configurations with AFWA's and uncover issues in the existing configurations, while the retrospective runs test individual changes.

This report covers the experimental design in Section 2, and discusses the data used in Section 3. Results from the real-time testing environment and the retrospective tests, which investigate the impact of the background error (BE) as well as data and model configuration impacts are covered in Section 4. Finally, a brief summary and concluding remarks are included in Section 5.

2. Experimental Design

a. Grid and domain

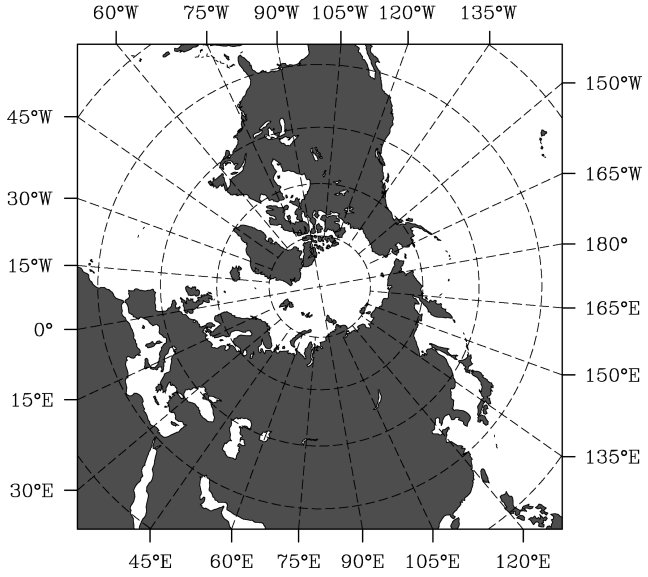

Figure 1: AFWA northern hemispheric domain used for DTC GSI baseline tests. Configured at 20 km horizontal resolution, 57 vertical sigma levels, and a 10 hPa model top. Also referred to as the T51 domain.

The DTC baseline tests follow the same grid setup as the AFWA parallel system. The testing domain is the AFWA northern hemisphere domain (Domain T51) (Fig 1), using a polar stereographic map projection. The model grids, in dimension of 751x751, have a 20 km horizontal resolution and 57 full vertical sigma levels with a 10 hPa model top.

b. DTC GSI-ARW system structure

The setup of the DTC end-to-end data assimilation and forecast system follows the cycling scheme provided by AFWA. The only differences between the current AFWA system and the DTC system are input fields and individual changes to be tested. The DTC uses the NCEP GFS analyses and forecasts and real-time SST data as background and boundary conditions, while AFWA uses UKMet files and AGRMET and TAVGSFC SST data.

The DTC system (Fig 2) includes two cycles: 06 Z cold start cycle and a 12 Z continuous cycle. The 06 Z cold start cycle starts with collecting background files, GFS 0-56 hour forecasts initiated at 06Z (GRIB2 files, 0.5° horizontal resolution) and real-time SST data from NCEP. The WRF preprocessing system (WPS and *real*) is then run to decode and interpolate data into the testing domain and grids. *real* is run twice; first to generate a background file for GSI, wrf_input, valid at 06 Z (GFS analysis) and boundary conditions valid from 06-12 Z, and a second time to generate the boundary files covering 48 hour forecasts starting from 12 Z. Next, GSI is run to generate an analysis using the background from the 06 Z GFS analysis and the observations within a ±3hour time window from the GFS PrepBUFR (for conventional observations) and BUFR files (for satellite observations)). For satellite data assimilation, GSI cycles the radiance bias correction by reading the radiance bias correction coefficients from the previous GSI cycle. The bias correction coefficients are then updated for angular bias correction. The boundaries conditions are then updated by *update_BC* using the GSI analyses and GFS forecasts. Finally, Advanced Research WRF (ARW) is run to generate 6 hour model forecasts.

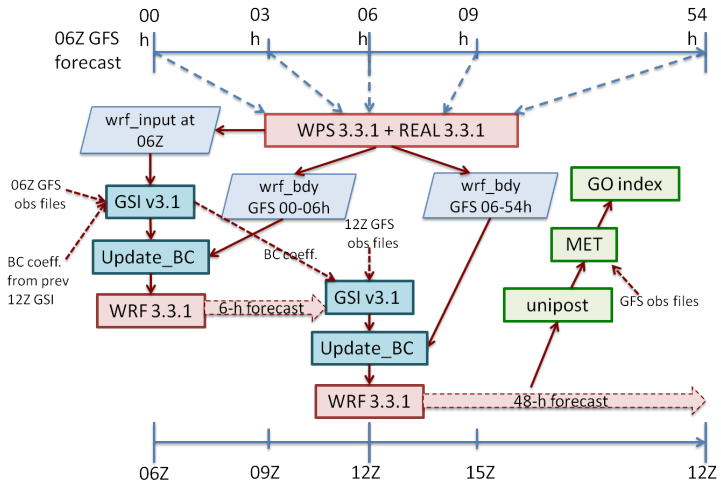

Figure 2: Schematic of DTC real-time system following the AFWA pre-operational configuration.

Unlike the 06Z cycle, the 12Z continuous cycle uses the 6 hour forecasts generated by the 06Z cycle as the background. Following the GSI run, the ARW is run to produce 48 hour forecasts for verification. The forecasts are processed by the Unified Post-Processing (UPP) system and verified by the Model Evaluation Tools (MET) against GFS PrepBUFR conventional data. Finally, AFWA GO-index statistics are generated based on MET statistics.

The versions of model components of the system are listed as follows:

- GSI: v3.1
- update_BC: 2012 version
- WRF: v3.3.1
- UPP: v1.0
- MET: v4.0

Appendix A provides relevant portions of the GSI namelist used in the DTC system. Appendix B provides relevant portions of the WRF-ARW namelist used in the DTC system.

c. Data

Table 1 summarizes the data linked, read into, and used in the analysis for both the DTC and AFWA systems. When building the DTC GSI configuration, channels and prepbufr observation types followed those of the AFWA system by matching convinfo and satinfo files.

Table 1: Data linked, read in, and used in the GSI analysis for both the AFWA and DTC systems.

Data file linked	Data type read in	Used in analysis
PREPBUFR	Read in: ps, t, q, uv	All
AIRS	Read in data from AQUA	used
AMSU-A	From N18, AQUA, N19	All used
HIR3	No N17 data read in; N16 turned off	
HIR4	From N19, METOP-A	Both used
SBUV/2	sbuv2 from n16, n17, n18, n19	None of data used
TRMM	No data read in	
GPSRO	Reads in: gps_ref	Used

There are a few main differences between the AFWA system and the DTC system. First, AFWA uses their own global model fields from the UKMET office, whereas DTC uses the GFS. Second, the DTC real-time tests are missing the AGRMET and TAVGSFC surface fields due to lack of availability of the data. Third, AFWA processes their observations, whereas the DTC is currently using NCEP prepbufr observations. Future plans include obtaining AFWA BUFR files for retrospective test cases.

3. GSI configuration

The results in the fit files were compared between a supplied AFWA test case and preliminary DTC configuration runs to check for differences in the analysis fit to the observations between the AFWA and DTC configurations (Table 2a,b). It is important to note that the AFWA and DTC files were not generated during the same cycle. The AFWA statistics were generated from 2012090712, which was a supplied case from AFWA, whereas the DTC statistics were generated during the 2012103112 cycle during the initial set-up of the DTC configuration. Both configurations were during the 12Z cycle, and are compared to gain a general feel for the differences in the analysis fit to observations. One noticeable difference is the lack of aircraft (131, 231) data in the NCEP prepbufr observations used in the DTC configuration. AFWA uses more observations overall. In general, the results are comparable, which indicates that the DTC GSI tests are functionally similar to the AFWA ones.

Table 2a: Fit comparison for convention data between AFWA and DTC configurations

Variable		**AFWA**	O-B	O-A	Reduce %	**DTC**	O-B	O-A	Reduce %
T	bias	36589	-0.23	-0.11		23160	-0.30	-0.11	
	rms		1.44	1.05	**27.1**		1.65	1.24	**24.8**
T-120	Bias	19738	-0.38	-0.23		20106	-0.28	-0.14	
	rms		1.56	1.23	**21.2**		1.63	1.22	**25.2**
T-131	bias	16080	-0.09	0.03		0			
	rms		1.20	0.67	**44.2**				
UV	bias	45128	0.19	0.34		31352	-0.02	0.27	
	rms		4.50	3.31	**26.4**		4.63	3.49	**24.6**
UV-220	bias	15239	0.15	0.37		22529	0.09	0.34	
	rms		4.31	3.25	**24.6**		4.78	3.61	**24.5**
UV-231	bias	15976	0.00	0.22		0			
	rms		4.52	3.24	**28.3**				
q	bias	10305	-1.44	-0.52		9817	-1.10	0.08	
	rms		16.57	11.29	**31.9**		16.08	12.39	**22.9**
q (120)	bias	9922	-1.52	-0.56		8930	0.05	0.05	
	rms		16.78	11.45	**31.8**		16.59	12.72	**23.3**
Ps (180,181,187)	bias	9412	-0.2031	-0.0009		29963	-0.2397	-0.0213	
	rms		1.1213	0.6334	**43.5**		1.0901	0.7925	**27.3**

Table 2b: Fit comparison for GPSRO data between AFWA and DTC configurations

GPS	**AFWA**	O-B	O-A	Reduce	**DTC**	O-B	O-A	Reduce
Bias	All	-0.29	-0.03		All	-0.17	-0.02	
RMSE	16472	0.73	0.36	**50.7**	11560	0.66	0.35	**47.0**
Bias	740	-0.32	-0.03		740	-0.10	0.0	
RMSE	3273	0.74	0.35	**52.7**	1367	0.62	0.35	**43.5**
Bias	741	-0.13	-0.03		741	-0.21	-0.03	
RMSE	4313	0.77	0.37	**51.9**	2365	0.73	0.38	**47.9**

4. Experiments and Results

a. Real-time system setup

The real-time setup of the DTC testing environment functionally similar to the AFWA PO configuration consists of two parallel real-time tests; the first (referred to as the primary configuration herein) acts as a consistent baseline test following the AFWA PO configuration, and the second (referred to as the developmental configuration herein) matches the primary configuration with incremental changes to test and monitor the data assimilation (DA) development activity. During the initial 2-week period of the real-time tests, the developmental run was a cold-start ARW forecast initialized using the GFS. This was done to test the baseline performance of the primary configuration and catch forecast impacts when changes were made to the system during the initial set-up. Figure 3 shows the GO-index for the primary run compared to the cold-start developmental run. A noticeable drop in the GO-index occurs on October 30, coinciding with the addition of the GPSRO data and the switch from the NAM BE to the GFS BE during the initial set-

up. Subsequent retrospective tests over this 2-week period were performed to pinpoint the reason for the drop in forecast skill.

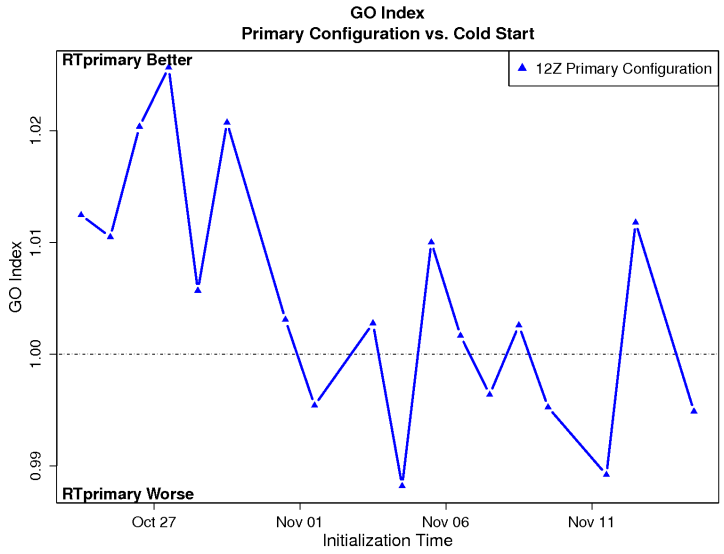

Figure 3: GO-index of primary configuration vs. the cold-start GFS run during a 2-week retrospective period from Oct 24 – Nov 9, 2012.

In addition to the GO-index, bias and RMSE scores were computed over the period of Oct 24 – Nov 9, 2012 for the 48-hour WRF forecasts generated at 12 Z for each cycle. These scores show statistically significant (SS) differences favoring the RTprimary (GSI) over the RTdev (noda), particularly at the earliest lead times and mid-levels (Fig 4).

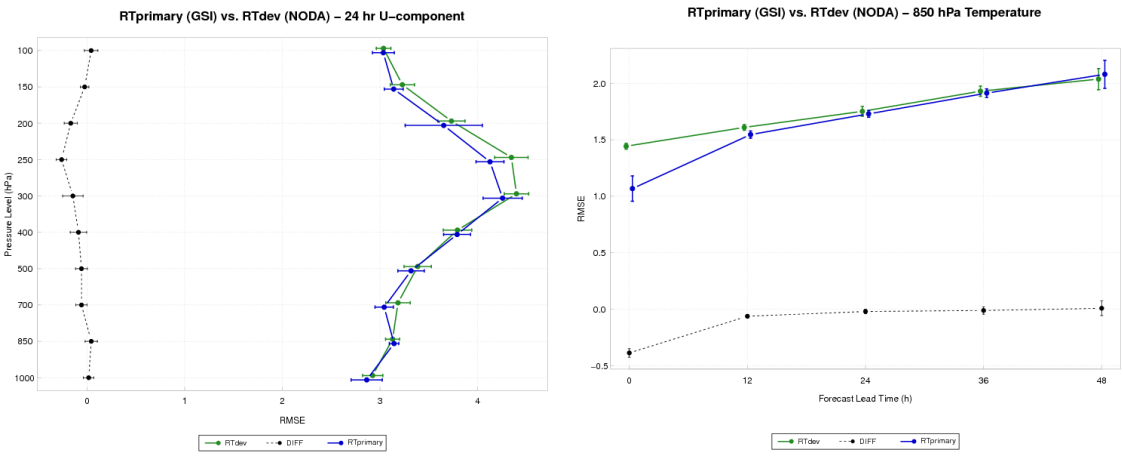

Figure 4: RMSE vertical profile for GSI (blue), NODA (green), and pair-wise difference (black) for the 24-hour ARW forecast U-component wind field (left) and 850 hPa temperature timeseries of RMSE for 0-48 hr lead times (right). SS difference is determined when the black confidence interval does not encompass zero.

These results show the DTC configuration following the AFWA PO configuration produces verification metrics over the forecast period that show more forecast skill than the GFS cold start run, with statistical significance at the 95% level.

b. BE Retrospective testing

In addition to the real-time configurations, short-term retrospective tests were performed over a 2-week period to test the impact of individual changes to the primary configuration.

i. Operational BE tests

After the real-time tests indicated a drop in skill (Fig 3), focus turned to additional retrospective tests to isolate the forecast impact stemming from the choice in BE for the T51 domain. Figure 4 shows the retrospective tests using the NAM BE, GFS BE (without GPSRO assimilated), and RAP BE. Results show the most positive impact of the forecast skill from the NAM BE.

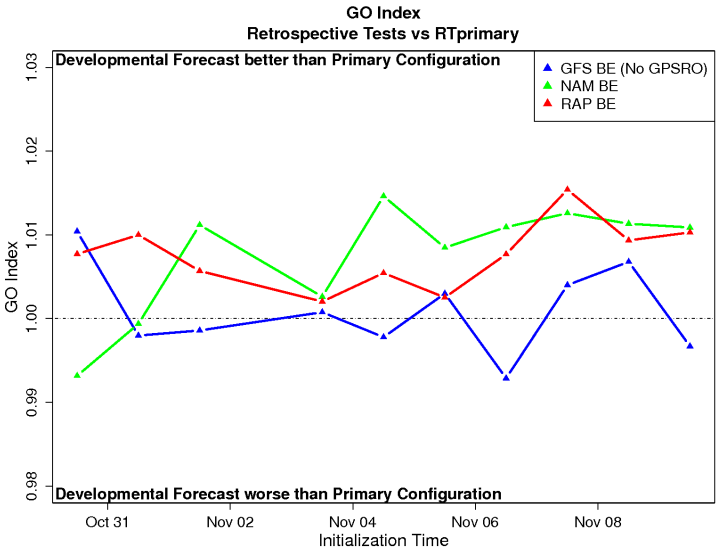

Figure 4: GO index of NAM (green), RAP (red), and GFS (blue) BE runs vs. primary configurations during a 2-week retrospective period.

Vertical RMSE profiles (Figures 5 a,b) during the analysis time show the analysis generated using the NAM BE fits the observations closer than the RAP and the GFS BE for wind (as well as dew point and height, not shown), with the analysis generated using the GFS BE fitting the observations closer for temperature.

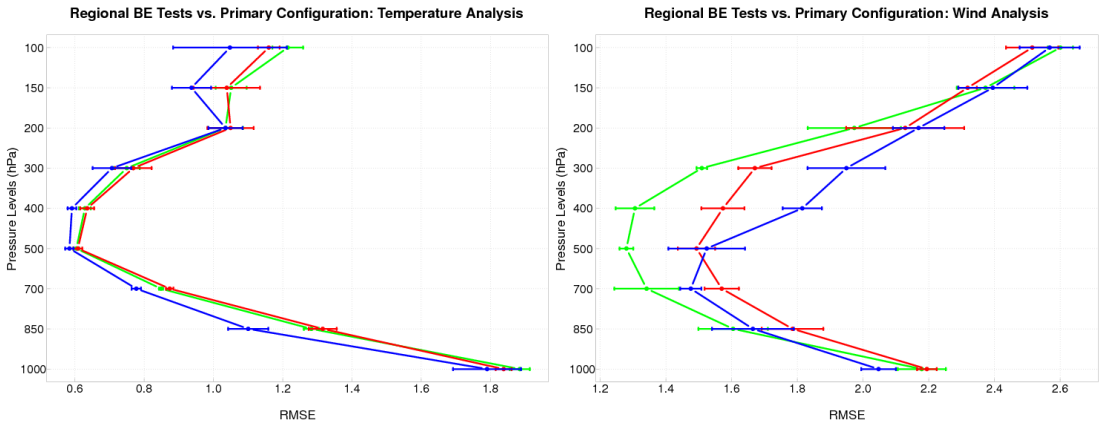

Figure 5: Vertical profiles of RMSE for Regional BE retrospective tests (NAM, green; RAP, red) vs. primary configuration (GFS, blue) at the analysis time. Temperature analysis on left (a); Wind analysis on right (b).

Pseudo-single observation tests (PSOT) were performed using the GFS and NAM BEs (Figure 6). A temperature increment was placed at 38°N, 81°W and 500 hPa. Results show the level of spatial extent and magnitudes are larger for GFS than NAM. This result gives a feel for the magnitude and spatial extent, which work best with this configuration (following NAM).

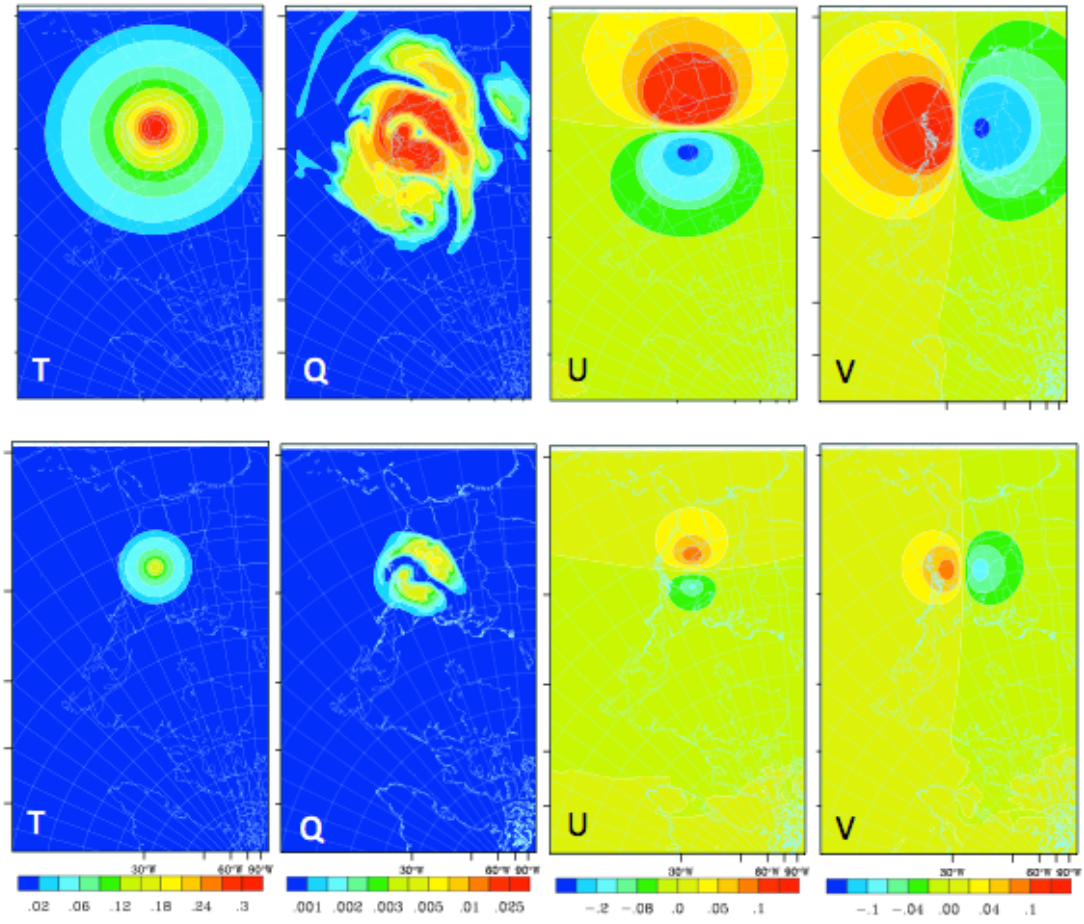

Figure 6: PSOT using GFS BE (upper) and NAM BE (lower) for T,Q,U,V (left to right).

ii. Domain-specific BE

A domain-specific BE was generated using forecasts collected from the primary configuration over the 3 month period of October – December 2012. The BE was generated by the GEN_BE-GSI code (Rizvi, 2010) using the NMC method (48 hr-24 hr). BE statistics and subsequent tuning have been performed using the T51 domain-specific BE. Figure 7 shows variance, horizontal length scale, and vertical length scale for NAM and the T51 domain-specific BE.

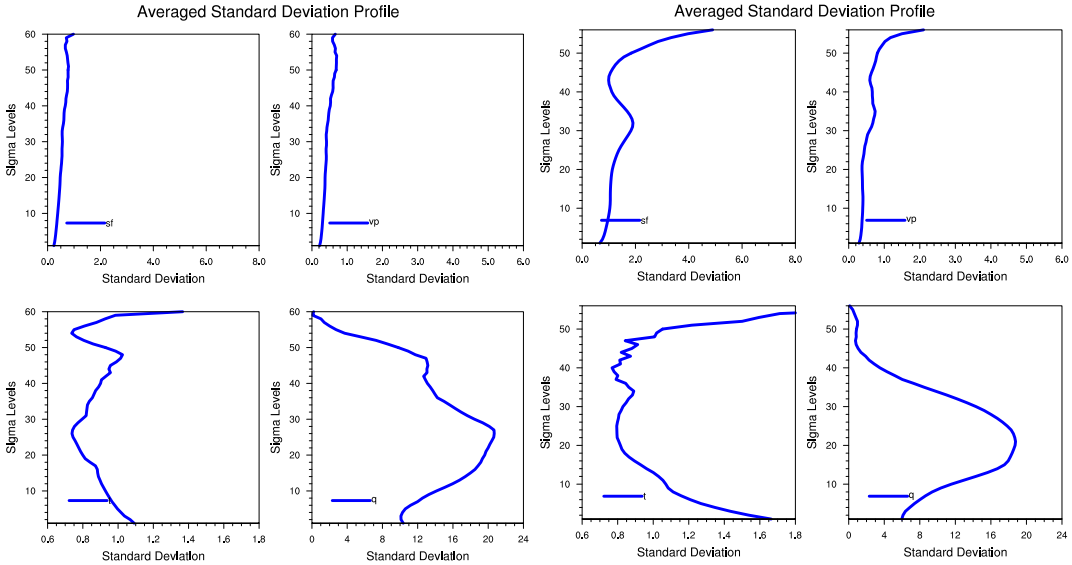

Figure 5a: Variance profiles for NAM BE (left) and T51 regional BE (right) for streamfunction, velocity potential, moisture, and temperature (clockwise).

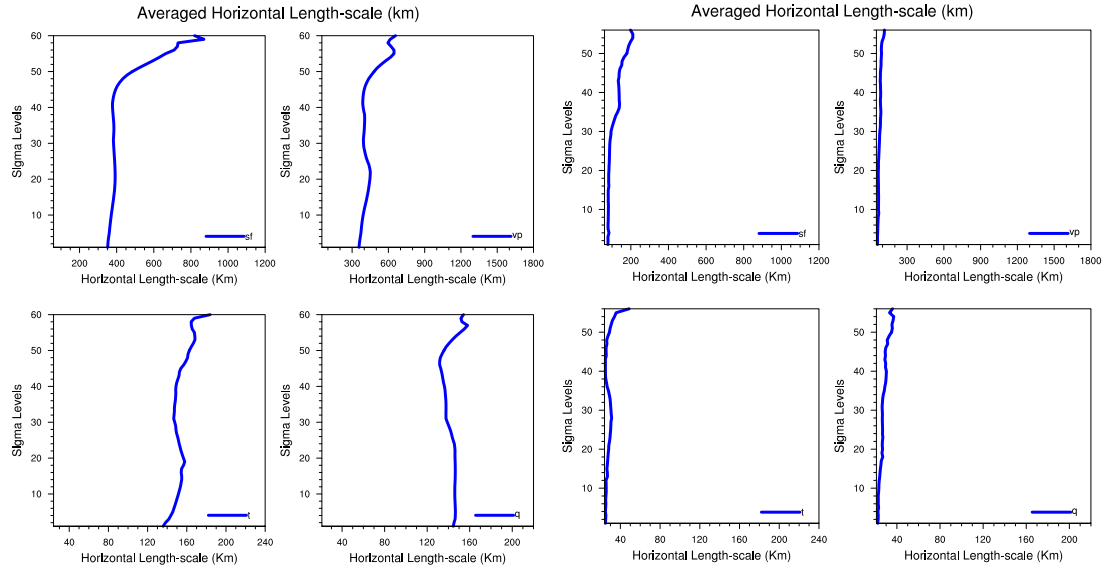

Figure 5b: Horizontal length scale profiles for NAM BE (left) and T51 regional BE (right) for streamfunction, velocity potential, moisture, and temperature (clockwise).

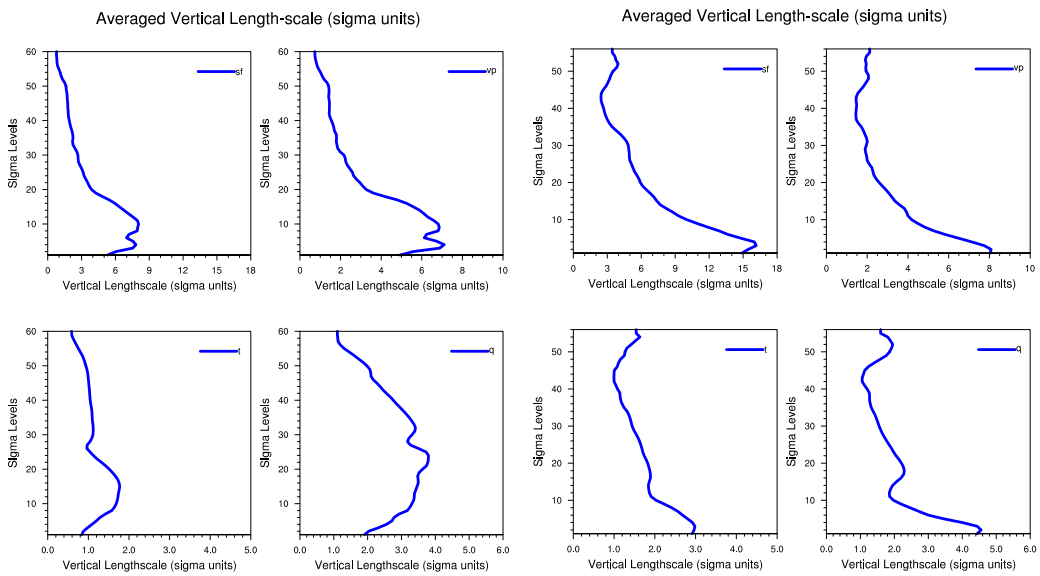

Figure 5c: Vertical length scale profiles for NAM BE (left) and T51 regional BE (right) for streamfunction, velocity potential, moisture, and temperature (clockwise).

Results show the domain-specific BE variances are fairly similar to those of the NAM BE, however the magnitudes of the horizontal length scale are significantly smaller than those of the NAM BE. Initial retrospective tests (Fig 8) show degradation to the forecast skill relative to the primary configuration when the T51 regional BE is used with no tuning. Figure 9 shows the GO index with two iterations in the T51 BE tuning. The first iteration (Tune A) is a BE generated with the balance part from the T51 domain-specific BE, and the horizontal and vertical length scales and variance using NAM statistics generated from GSI. The second tuned BE (Tune B) is the NAM BE interpolated onto the T51 grid. Results show bringing the BE closer to the NAM skill, but work is still in progress to further tune this BE for this application. Current guidance is to use the NAM BE for application in the northern hemisphere.

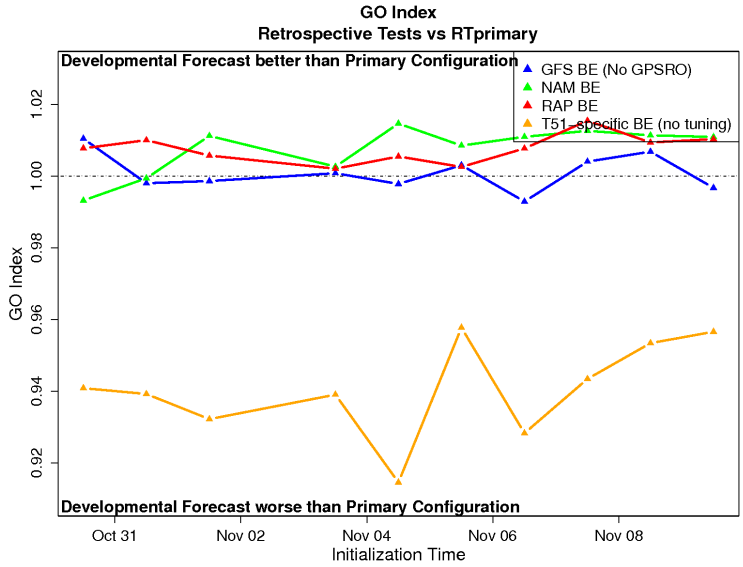

Figure 8: GO index of NAM (green), RAP (red), GFS (blue), and T51 domain-specific (no tuning) BE runs vs. primary configurations during a 2-week retrospective period.

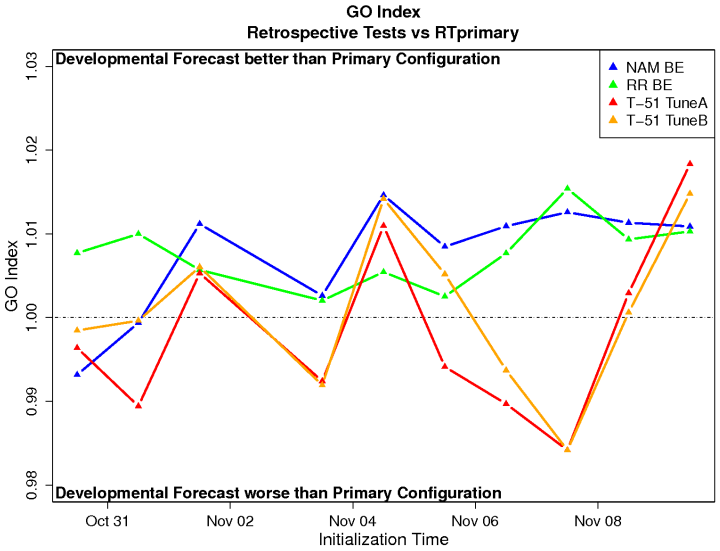

Figure 9: GO index of NAM (blue), RAP (green), and two iterations of T51 tuned (red, orange) BE runs vs. primary configurations during a 2-week retrospective period.

Further tests on Tune B show potential issues with the generation of this tuned BE in the vertical interpolation. Plots show skill of the Tune B BE degrading with height compared to the skill of the NAM BE. This result indicates further work needs to be done in the generation and tuning of the domain-specific regional BE.

c. Data impact

i. GPSRO

Additional testing was performed to determine the impact of the GPSRO data on the forecast skill over T51. GPSRO results (Fig 10) show neutral improvement. Although the result was neutral, variability in the result suggested that GPSRO could provide improvements if tuning was performed for the regional domain (current GPSRO is tuned for global models).

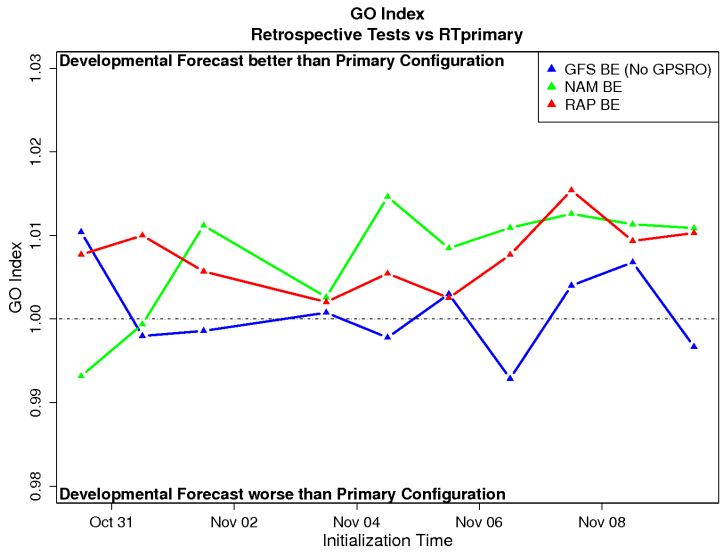

Figure 10: GO index of NAM (blue), RAP (green), and GFS (blue) BE runs vs. primary configurations during a 2-week retrospective period. The blue line shows difference between GFS retrospective test vs. primary configuration run, where the only difference is the inclusion of the GPSRO data.

ii. Channel Selection

The impact of using channel selection to reduce the number of channels assimilated for radiances was tested based on research preformed by GSI research colleagues at NOAA/GSD/AMB working on the RAP system (Lin, 2012). Initial research showed promising improvement to upper level forecast skill when performing channel selection with continuous cycling. Table 3 shows the channels used after the reduction to the radiance data assimilation in the primary configuration.

Table 3: Channels used after channel selection

Radiance data		Channels Used
AMSU-A	noaa-17	Ch1-10,15
	noaa-19	Ch 1-7,9-10,15
	AQUA	Ch 6,8,9-10
HIR4	noaa-19	Ch 4-8,10-15
	METOP-A	Ch 4-8, 10-15
AIRS	AQUA	68 channels *(reduced from 120)*

Although channel selection provided positive results for research colleagues, the results over the T51 domain provide neutral results (Fig 11), with no statistically significant results favoring either configuration. This result may stem from the cold-start cycling scheme used, or could highlight the overall impact of radiance data assimilation for this configuration.

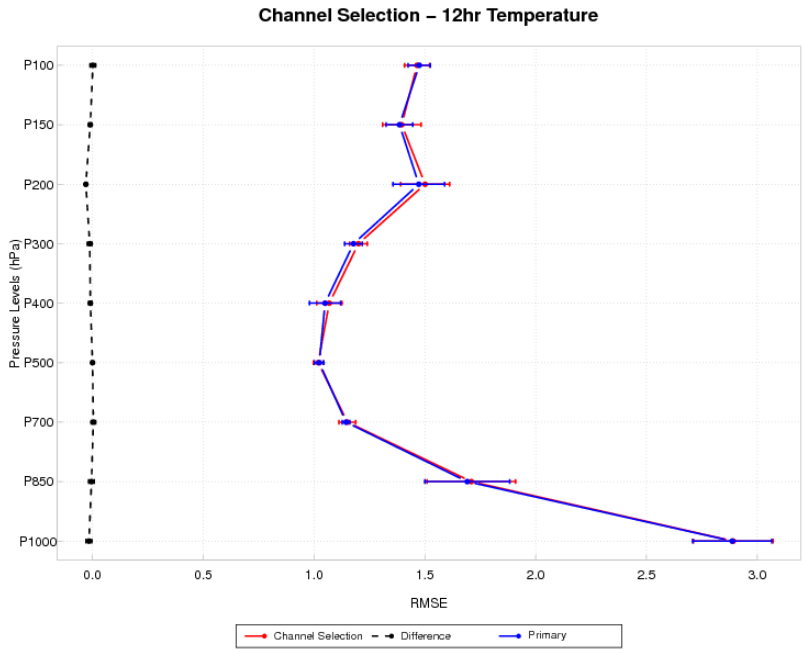

Figure 11: Vertical profile of RMSE for channel selection test. The blue line represents the primary configuration, the red line represents the channel selection test performed in the developmental configuration, and the black line shows the pair-wise statistically significant differences between the two tests (95%).

d. Regional BE generation methods

In addition to the real-time configuration tests and BE retrospective tests, testing for regional BE generation methods was also conducted. Specifically, work has been done to look at the differences between the NMC method vs. the Ensemble BE method, both available within the GEN_BE-GSI utility. For both the NMC and Ensemble BE generation, ARW forecasts were obtained from the FY2011 AFWA EnKF testbed (Fig 12). The model was configured with a 36-km horizontal resolution, 45 vertical levels, and a 20 hPa model top.

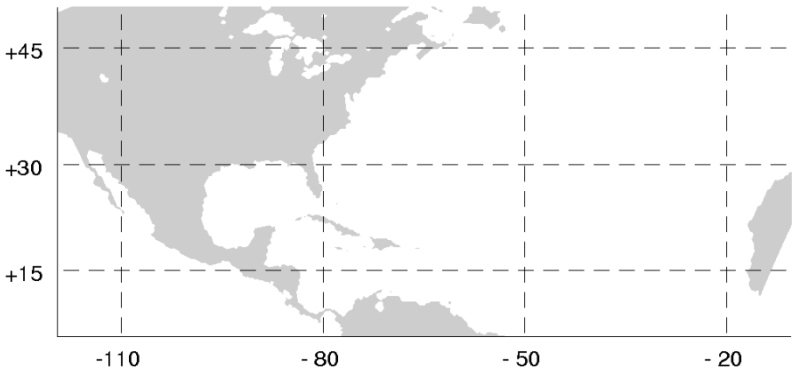

Figure 10: Computational domain used for FY2011 AFWA EnKF testing.

The deterministic forecasts from 2008081100 through 2008091312 were used to generate a regional BE using the NMC method (48h-24h) and compared against the global BE (Fig 13).

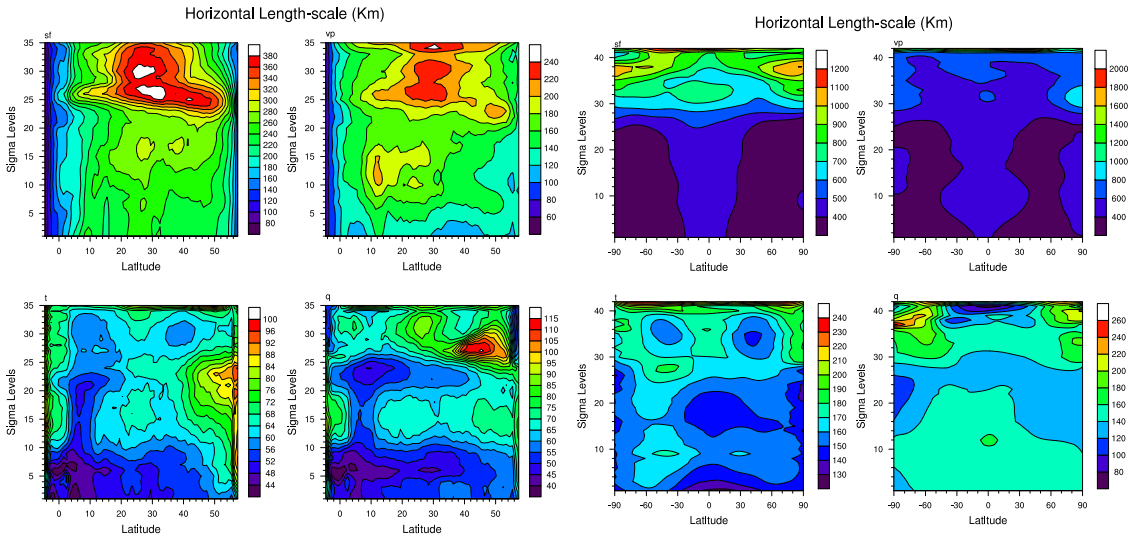

Figure 13a: Horizontal length scales for regional (NMC) BE (left) and global BE (right). Panels are stream function, velocity potential, moisture, temperature (clockwise from top left).

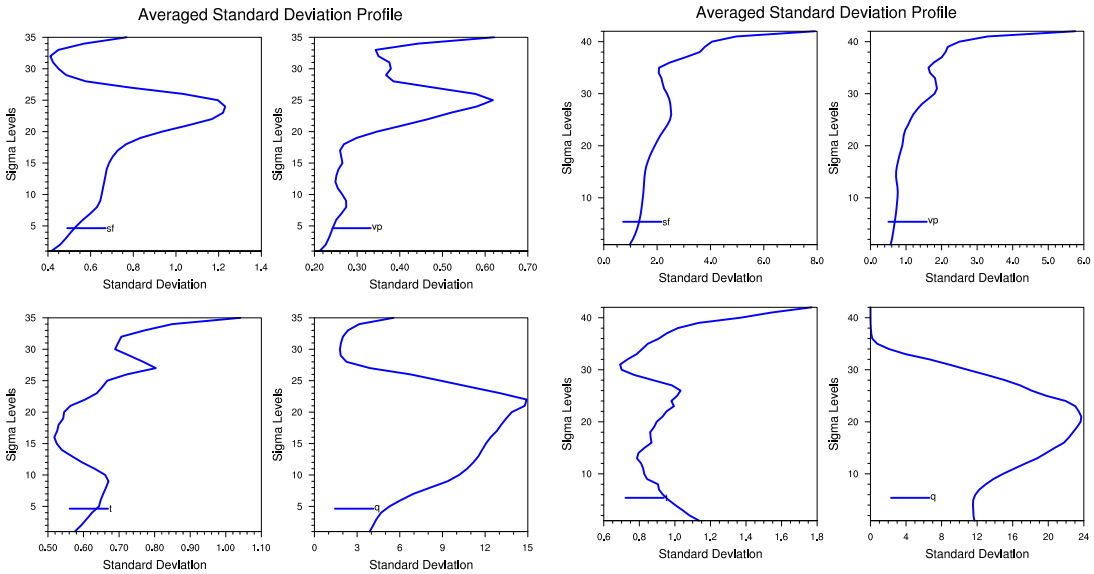

Figure 13b: Averaged standard deviation profile for regional (NMC) BE and global BE (right). Panels are stream function, velocity potential, moisture, and temperature (clockwise from top left).

A noticeable feature in the regional NMC method horizontal length scale (Fig 13a) is the noise near the boundaries. The model top may also provide issues with the regional BE shown by the average standard deviation profile spike near the top of the model (Fig 13b).

In addition to the NMC method, the ensemble (ENS) method was also used to generate a regional BE using ensemble forecasts from the FY2011 AFWA EnKF

testbed (Fig 10). Six-hour ensemble forecasts valid at 2008081106 and 2008081112 were used for BE generation, with 96 ensemble members for each valid time. Figure 14 shows the ensemble BE diagnostics compared to those generated using the NMC method on the deterministic forecasts.

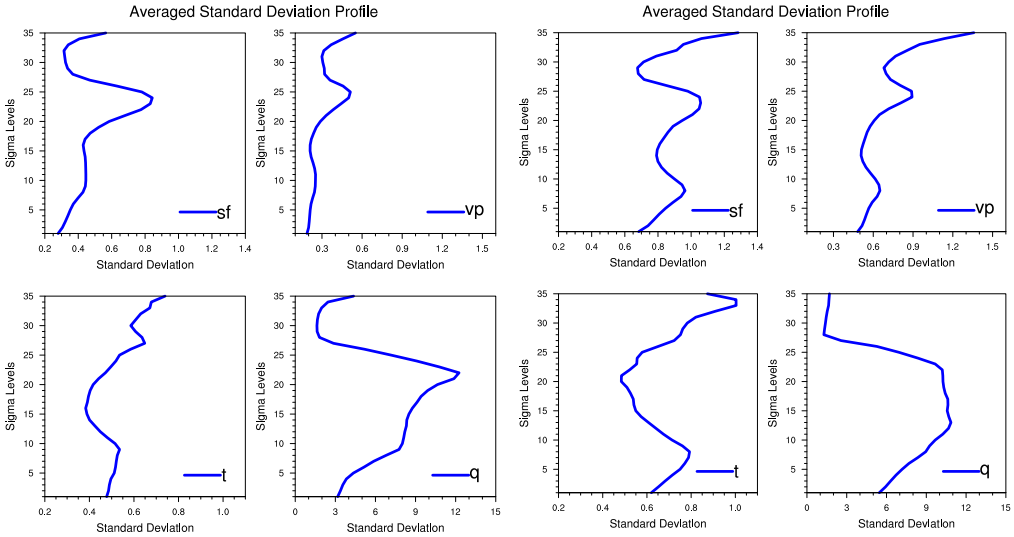

Figure 14a: Average standard deviation profile for NMC BE (left) and ENS BE (right). Panels are stream function, velocity potential, moisture, temperature (clockwise from top left).

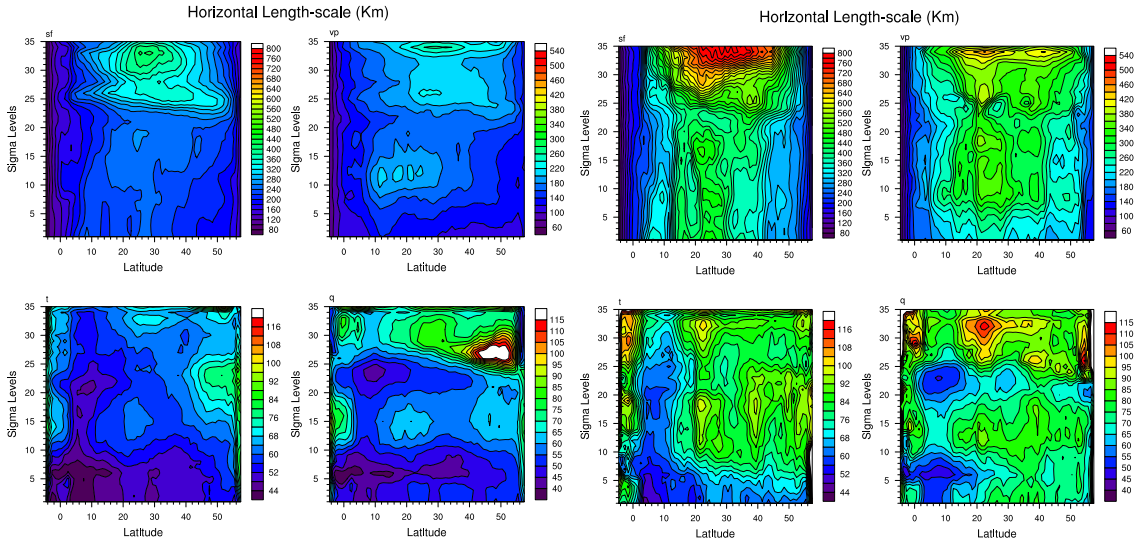

Figure 14b: Horizontal length scales for NMC BE (left) and ENS BE (right). Panels are stream function, velocity potential, moisture, temperature (clockwise from top left).

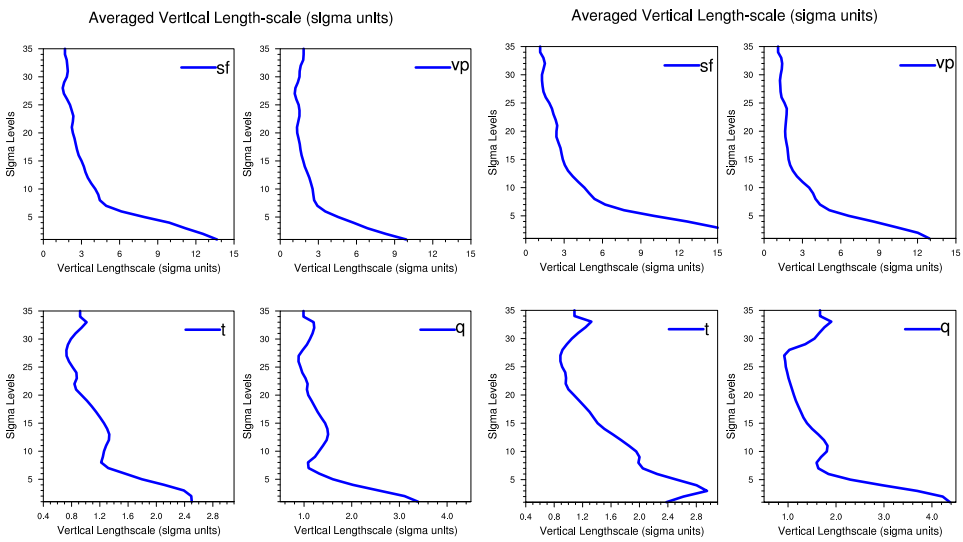

Figure 14c: Average vertical length scale profile for NMC BE (left) and ENS BE (right). Panels are stream function, velocity potential, moisture, temperature (clockwise from top left).

Background error statistics show the ENS BE has larger variance, particularly true with the velocity potential. Horizontal and vertical length scale plots (Fig 14b,c) indicates the ENS BE has larger magnitude than the NMC BE for the horizontal length scale, and is fairly similar for the vertical length scales. Both the ENS and the NMC BEs show noise at the boundaries and model top, as seen in the horizontal length scale figure. Although the magnitude for the ENS BE is generally larger, the magnitude is still much smaller than the values seen with the global BE (Fig 13a,b).

In addition to the BE statistic, pseudo-single observation tests (PSOT) were run with both the NMC and ENS BEs in order to see the response of each BE in the GSI system. Figure 15 shows the PSOTs for a temperature increment placed at 38°N, 81°W, 500 hPa for both the NMC (a) and the ENS (b) methods.

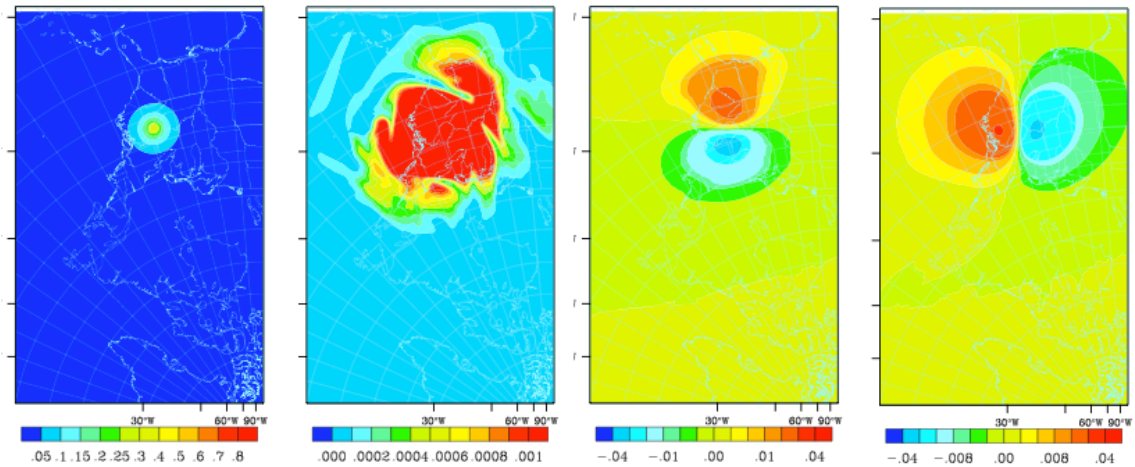

Figure 15a: PSOT response from a T increment at 500 mb using ENS BE T,Q,U,V (left to right).

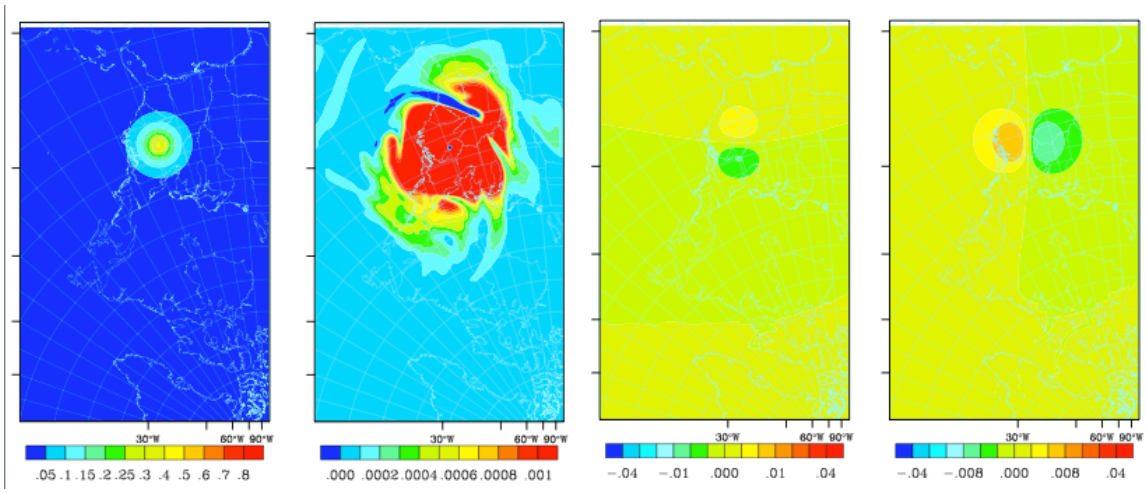

Figure 15b: PSOT response from a T increment at 500 mb using NMC BE T,Q,U,V (left to right).

The PSOT tests showed the ENS BE has a slightly smaller temperature increment, with a larger response in both magnitude and spatial extent than that of the NMC method. The moisture increment between the ENS and NMC BE PSOTs showed a very similar response.

5. Conclusions

The DTC has built and configured a functionally similar testing environment to the PO AFWA system. Initial tests show the primary configuration was performing better than the cold start GFS run, however during the implementation of the AFWA configuration, a noticeable drop in skill occurred during the addition of the GPSRO data and the switch from the NAM BE to the GFS BE. Subsequent 2-week retrospective tests displayed the cause of the drop was due to the BE change. Further testing of the GFS BE, NAM BE, RAP BE, as well as a domain-specific BE generated using 3 months of collected primary forecasts, shows the best solution for this particular configuration is the NAM BE. This recommendation was formed over the T51 domain, but should hold for any northern hemispheric domain with a similar configuration to T51. Further work is being done to provide a domain-specific BE with improved forecast skill.

Impact studies were done for the GPSRO and radiance assimilation. The GPSRO shows neutral improvement, but due to a response in the skill from adding GPSRO data, it is believed that improvement may be obtainable with regional tuning (GPSRO assimilation is currently tuned for global applications). Channel selection testing was performed following previous research conducted by GSI research colleagues. Initial tests indicated neutral improvement as well when comparing the two real-time runs. This may be due to the cycling scheme (initial tests were done with a full cycling rather than a partial cycling scheme), or could point to overall impact of radiance assimilation for this configuration.

Initial work was done using the FY2011 EnKF testing domain to compare the GEN_BE-GSI results when using the NMC method vs. the ensemble BE method. Results show the ENS BE results in a slightly larger variance and horizontal length scale. The vertical

length scales between the two methods are very similar. The PSOTs for both the ENS and NMC methods showed the U and V wind fields resulted in a much larger increment both spatially and in magnitude with the ENS method compared to the NMC method.

References

Lin, H., personal communication, 2012.

Rizvi, S. R. H., Z. Liu and X.-Y. Huang (2010): Generation of WRF-ARW background errors (BE) for GSI. AFWA 2010, mid term review report available at:

https://wiki.ucar.edu/download/attachments/50663734/WRF-ARW-GSI_BE.pdf

Appendix A: GSI namelist

```
&SETUP
  miter=2,niter(1)=50,niter(2)=50,
  write_diag(1)=.true.,write_diag(2)=.false.,write_diag(3)=.true.,
  gencode=78,qoption=2,
  factqmin=0.0,factqmax=0.0,deltim=1200,
  ndat=77,iguess=-1,
  oneobtest=.false.,retrieval=.false.,
  nhr_assimilation=3,l_foto=.false.,
  use_pbl=.false.,
 /
 &GRIDOPTS
  JCAP=62,JCAP_B=62,NLAT=,NLON=,nsig=60,hybrid=.true.,
  wrf_nmm_regional=.false.,wrf_mass_regional=.true.,
  diagnostic_reg=.false.,
  filled_grid=.false.,half_grid=.true.,netcdf=.true.,
 /
 &BKGERR
  vs=0.7,
  hzscl=1.7,0.8,0.5,
  bw=0.,fstat=.true.,
 /
 &ANBKGERR
  anisotropic=.false.,an_vs=1.0,ngauss=1,
  an_flen_u=-5.,an_flen_t=3.,an_flen_z=-200.,
  ifilt_ord=2,npass=3,normal=-200,grid_ratio=4.,nord_f2a=4,
 /
 &JCOPTS
 /
 &STRONGOPTS
  jcstrong=.false.,jcstrong_option=3,nstrong=0,nvmodes_keep=20,period_max=3.,
  baldiag_full=.true.,baldiag_inc=.true.,
 /
 &OBSQC
  dfact=0.75,dfact1=3.0,noiqc=.false.,c_varqc=0.02,vadfile='prepbufr',
 /
```

Appendix B: WRF –ARW namelist.input

```
&domains
 time_step                  = 60,
 time_step_fract_num             = 0,
 time_step_fract_den             = 1,
 max_dom                    = 1,
 s_we                       = 1,     1,     1,
 e_we                       = 751, 321, 157,
 s_sn                       = 1,     1,     1,
 e_sn                       = 751, 301, 154,
 s_vert                     = 1,     1,     1,
 e_vert                     = 57,    51,    51,
 num_metgrid_levels              = 27,
 num_metgrid_soil_levels         = 4,
 dx                         = 20000.0, 3000.0, 1000.0,
 dy                         = 20000.0, 3000.0, 1000.0,
 grid_id                    = 1,     2,     3,
 parent_id                  = 0,     1,     2,
 i_parent_start             = 0,  153,  166,
 j_parent_start             = 0,  159,  141,
 parent_grid_ratio          = 1,  4,3,
 parent_time_step_ratio          = 1,  3,3,
 feedback                   = 0,
 smooth_option              = 0
 p_top_requested            = 1000
 interp_type                = 1
 lowest_lev_from_sfc             = .false.
 lagrange_order             = 1
 force_sfc_in_vinterp       = 6
 zap_close_levels           = 500
 eta_levels = 1.000, 0.997, 0.992, 0.985, 0.978, 0.969, 0.960, 0.950,
       0.938, 0.925, 0.910, 0.894, 0.876, 0.857, 0.835, 0.812,
       0.787, 0.760, 0.731, 0.700, 0.668, 0.635, 0.600, 0.565,
       0.530, 0.494, 0.458, 0.423, 0.388, 0.355, 0.323, 0.293,
       0.264, 0.237, 0.212, 0.188, 0.167, 0.147, 0.130, 0.114,
       0.099, 0.086, 0.074, 0.064, 0.054, 0.046, 0.039, 0.032,
       0.027, 0.022, 0.017, 0.013, 0.010, 0.007, 0.004, 0.002,
       0.000,
/
&physics
 mp_physics                 = 4,     6,     6,
 ra_lw_physics              = 1,     1,     1,
 ra_sw_physics              = 1,     1,     1,
 radt                       = 30,    30,    30,
 sf_sfclay_physics          = 1,     1,     1,
 sf_surface_physics         = 2,     3,     3,
 bl_pbl_physics             = 1,     1,     1,
 bldt                       = 0,     0,     0,
 cu_physics                 = 1,     1,     0,
 cudt                       = 5,
 isfflx                     = 1,
 ifsnow                     = 0,
 icloud                     = 1,
 surface_input_source       = 1,
```

```
 num_soil_layers                  = 4,
 mp_zero_out                      = 2,
 maxiens                         = 1,
 maxens                          = 3,
 maxens2                          = 3,
 maxens3                          = 16,
 ensdim                          = 144,
 num_land_cat                     = 28,
 fractional_seaice                = 1,
 seaice_threshold                 = 271,
 tice2tsk_if2cold                 = .true.,
 /
&dynamics
 rk_ord                          = 3,
 diff_6th_opt                     = 2,
 diff_6th_factor                  = 0.10,
 w_damping                        = 1,
 diff_opt                        = 1,
 km_opt                           = 4,
 damp_opt                         = 3,
 base_temp                        = 283.,
 iso_temp                         = 210.,
 zdamp                           = 5000.,  5000.,  5000.,
 dampcoef                         = 0.05,    0.02,   0.01
 khdif                           = 0,      0,      0,
 kvdif                           = 0,      0,      0,
 SMDIV                            = 0.1,    0.1,    0.1,
 EMDIV                            = 0.01,   0.01,   0.01,
 EPSSM                            = 0.1,    0.1,    0.1
 non_hydrostatic                  = .true., .true., .true.,
 TIME_STEP_SOUND                  = 0,      4,      4,
 H_MOM_ADV_ORDER                  = 5,      5,      5,
 V_MOM_ADV_ORDER                  = 3,      3,      3,
 H_SCA_ADV_ORDER                  = 5,      5,      5,
 V_SCA_ADV_ORDER                  = 3,      3,      3,
 moist_adv_opt                    = 1,      2,      2,
 scalar_adv_opt                   = 0,      2,      2,
 chem_adv_opt                     = 0,
 tke_adv_opt                      = 0,
 use_baseparam_fr_nml             = .true.,
 /
&bdy_control
 spec_bdy_width                   = 5,
 spec_zone                       = 1,
 relax_zone                      = 4,
 specified                       = .true.,
 periodic_x                       = .false.,
 symmetric_xs                     = .false.,
 symmetric_xe                     = .false.,
 open_xs                         = .false.,
 open_xe                         = .false.,
 periodic_y                       = .false.,
 symmetric_ys                     = .false.,
 symmetric_ye                     = .false.,
 open_ys                         = .false.,
 open_ye                         = .false.,
```

```
nested                  = .false.,
/
```